Advanced Quantum Technologies

ADVANCED QUANTUM TECHNOLOGIES
www.advquantumtech.com

RESEARCH ARTICLE OPEN ACCESS

Preserving Quantum Coherence in Thermal Noisy Systems Via Qubit Frequency Modulation

Mahshid Khazaei Shadfar[1,2] | Farzam Nosrati[1,3] | Ali Mortezapour[4] | Vincenzo Macrì[1,5] | Roberto Morandotti[2] | Rosario Lo Franco[1]

[1]Dipartimento di Ingegneria, Università di Palermo, Palermo, Italy | [2]INRS-EMT, Québec, Canada | [3]IMDEA Networks Institute, Madrid, Spain | [4]Department of Physics, University of Guilan, Rasht, Iran | [5]Dipartimento di Fisica, Università di Pavia, Pavia, Italy

Correspondence: Mahshid Khazaei Shadfar (mahshid.shadfar@gmail.com) | Ali Mortezapour (mortezapour@guilan.ac.ir) | Rosario Lo Franco (rosario.lofranco@unipa.it)

Received: 26 March 2026 | **Revised:** 28 May 2026 | **Accepted:** 9 June 2026

Keywords: dephasing | physics | quantum decoherence | quantum mechanics | quantum technology | quantum | qubit

ABSTRACT

Quantum coherence is a key resource underpinning quantum technologies, yet it is highly susceptible to environmental decoherence, especially in thermal settings. While frequency modulation (FM) has shown promise in preserving coherence at zero temperature, its effectiveness in realistic, noisy thermal environments remains unclear. In this work, we investigate a single frequency-modulated qubit interacting with a thermal phase-covariant reservoir composed of dissipative and dephasing channels. We demonstrate that FM significantly preserves coherence in the presence of thermal dissipation while being ineffective under thermal pure-dephasing noise due to commutation between system and interaction Hamiltonians. When both noise channels are present, FM offers protection only for weak dephasing coupling. Our findings clarify the limitations and potential of FM-based coherence protection under thermal noise, supplying practical insights into designing robust quantum systems for quantum applications.

1 | Introduction

Quantum coherence, a direct consequence of the superposition principle, is a fundamental aspect of quantum mechanics that sets it apart from classical mechanics [1–11]. Beyond its foundational significance, quantum coherence is also a crucial resource for various quantum technologies and protocols [12–19]. These include quantum metrology [20–22], nonclassicality measures [3, 23], quantum dense coding [24], quantum error correction (QEC) [25, 26], quantum key distribution (QKD) [27], quantum computing [28, 29], and quantum thermalization processes [30, 31]. By leveraging quantum coherence, these protocols can enhance precision [21, 32–41] and computational efficiency [42, 43].

However, in realistic settings, any quantum system inevitably interacts with its surrounding environment, leading to decoherence, that is the degradation of coherence due to the loss of phase information between components of a quantum superposition [44–46]. Numerous strategies have been proposed to mitigate decoherence and protect quantum coherence [29, 47–57]. Among these, frequency modulation (FM) of the qubit's transition frequency has emerged as a promising signal-processing technique for decoherence suppression. In this approach, the qubit's transition frequency ω_0 is modulated sinusoidally by an external off-resonant field [58–66], which can effectively decouple the system from its reservoir.

Recent studies have shown that frequency-modulated qubits exhibit a rich variety of quantum phenomena, including the dynamic Stark effect [67], Landau-Zener–Stückelberg interference [68], enhanced non-Markovianity [69], topological transitions [70], and population trapping

[71], highlighting the increasing relevance of this technique.

Most quantum protection schemes have been investigated under the assumption of zero temperature, where thermal noise is absent [48, 49, 72, 73]. However, in practical scenarios, quantum systems operate at nonzero temperatures. For example, superconducting qubits [74, 75] and quantum networks [76, 77] are subject to thermal fluctuations, making it essential to design coherence-preserving techniques that remain effective in thermal environments. While frequency modulation has demonstrated efficacy in preserving coherence at zero temperature, its performance under thermal noise remains to be further investigated.

In this work, we explore the dynamics of a frequency-modulated qubit interacting with a thermal, phase-covariant reservoir, encompassing both dissipative and dephasing processes. First, we analyze a scenario where the qubit couples to a thermal dissipative reservoir at temperature T_1. We show that frequency modulation significantly prolongs coherence even at elevated temperatures compared to the undriven case. Next, we investigate a qubit coupled to a pure-dephasing reservoir at temperature T_2. In this case, frequency modulation is found to be completely ineffective due to the commutation between the qubit's self-Hamiltonian and the interaction Hamiltonian. Finally, we consider a more general scenario where the qubit interacts independently with both a thermal dissipative and a thermal dephasing reservoir. Our results reveal that frequency modulation can still protect quantum coherence, but only if the dephasing coupling strength α remains below a certain threshold. We also identify the critical value of α beyond which frequency modulation no longer offers protection.

The paper is organized as follows. In Section 2 we present a general model to describe the dynamics of a frequency-modulated qubit undergoing phase-covariant noise, using a time-local master equation. Section 3 and Section 4 report the results that demonstrate the effectiveness of FM in preserving quantum coherence of the qubit under different noisy conditions. Finally, we outline main conclusions and prospects in Section 5.

2 | Model

The system under consideration is a qubit (two-level system), with an excited state $|e\rangle$ and a ground state $|g\rangle$. The qubit transition frequency ω_0 is modulated sinusoidally by an external driving field, characterized by a modulation amplitude δ and a modulation frequency Ω ($\delta, \Omega \ll \omega_0$). The qubit interacts with two independent types of ideal noise: amplitude damping noise and phase noise at temperature T_1 and T_2, respectively, as depicted in Figure 1. The term ideal means that the noise is sufficiently weak and random [78]. Each noise source can be modeled as a reservoir composed of an infinite array of random, broad-spectrum harmonic oscillators [44]. The total Hamiltonian for a driven qubit coupled to two local reservoirs (noise sources) can be written as

$$H = H_{\mathrm{q}} + H_{\mathrm{r1}} + H_{\mathrm{r2}} + H_{\mathrm{I,dis}} + H_{\mathrm{I,deph}}, \tag{1}$$

where H_{q} is the Hamiltonian of the driven qubit ($\hbar = 1$)

$$H_{\mathrm{q}} = \frac{\hbar}{2}(\omega_0 + \delta\cos(\Omega t))\sigma_z, \tag{2}$$

with σ_z denoting the Pauli operator along the z-direction; $H_{\mathrm{r1}} = \sum_k \omega_k a_k^\dagger a_k$ and $H_{\mathrm{r2}} = \sum_l \mu_l b_l^\dagger b_l$ are the Hamiltonians of the reservoirs, where, $a_k^\dagger, b_l^\dagger$ (a_k, b_l) are the creation (annihilation) operators of the damping reservoir mode k with frequency ω_k and dephasing reservoir mode l with frequency μ_l, respectively. $H_{\mathrm{I,dis}}$ ($H_{\mathrm{I,deph}}$) describes the interaction between the qubit and the dissipative (dephasing) reservoir modes

$$H_{\mathrm{I,dis}} = \sum_k \left(g_k\sigma_+ a_k + g_k^* a_k^\dagger \sigma_-\right), \tag{3}$$

$$H_{\mathrm{I,deph}} = \sum_l \sigma_z\left(f_l^* b_l^\dagger + f_l b_l\right), \tag{4}$$

where g_k (f_l) are the coupling constant between the qubit and mode k (l), while the operators $\sigma_\pm = \sigma_x \pm i\sigma_y$ are the qubit raising and lowering operators.

The time-local master equation for this qubit, derived after tracing over the two reservoirs and considering phase-covariant noise in the interaction picture, is expressed as (see Appendix A and C for a detailed derivation)

$$\begin{aligned}\dot{\rho}_q(t) = &-i\omega(t)[\sigma_z, \rho_q(t)] + \frac{\gamma_1(t)}{2}\mathbf{L}_1[\rho_q] \\ &+ \frac{\gamma_2(t)}{2}\mathbf{L}_2[\rho_q] + \frac{\gamma_3(t)}{2}\mathbf{L}_3[\rho_q],\end{aligned} \tag{5}$$

where $\omega(t) = \frac{\hbar}{2}(\omega_0 + \delta\cos(\Omega t))$ is the modulated transition frequency [61], and $\gamma_i(t)$ ($i = 1, 2, 3$) are the time-dependent rates associated with the Lindbladian superoperators $\mathbf{L}_i[\rho_q]$. These superoperators are defined as [79–81]

$$\begin{aligned}\mathbf{L}_1[\rho_q] &= \sigma_-\rho_q(t)\sigma_+ - \frac{1}{2}\sigma_+\sigma_-\rho_q(t) - \frac{1}{2}\rho_q(t)\sigma_+\sigma_-, \\ \mathbf{L}_2[\rho_q] &= \sigma_+\rho_q(t)\sigma_- - \frac{1}{2}\sigma_-\sigma_+\rho_q(t) - \frac{1}{2}\rho_q(t)\sigma_-\sigma_+, \\ \mathbf{L}_3[\rho_q] &= \sigma_z\rho_q(t)\sigma_z - \rho_q(t),\end{aligned} \tag{6}$$

The three superoperators $\mathbf{L}_1, \mathbf{L}_2$, and $\mathbf{L}_3$, describe dissipation, heating, and dephasing, respectively. The time-local master equation for this qubit combines the effects of a pure-dephasing reservoir when $\gamma_1(t) = \gamma_2(t) = 0$ and a dissipative reservoir when $\gamma_3(t) = 0$ [79–81]. The bath temperatures are meant to be included in the general time-dependent noise rates $\gamma_i(t)$, as we shall report in the next section.

The solution of this master equation, expressed in the basis $\{|e\rangle, |g\rangle\}$, is represented as the qubit density matrix

$$\rho_{\mathrm{q}}(t) = \begin{pmatrix} 1 - P_g(t) & \zeta(t) \\ \zeta^*(t) & P_g(t)\end{pmatrix}, \tag{7}$$

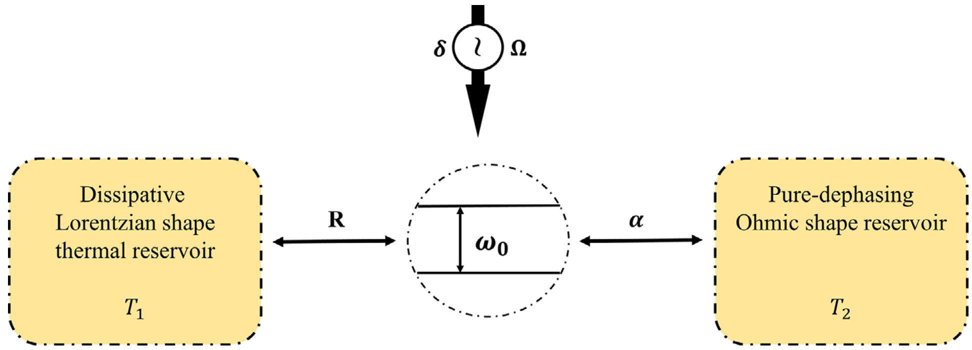

FIGURE 1 | A sketch of the driven qubit system. A qubit (two-level atom) interacts with two independent types of ideal noise: dissipative noise at temperature T_1 and phase noise at temperature T_2. The transition frequency of the qubit ω_0 is modulated sinusoidally by an externally applied field, characterized by a modulation amplitude δ and a modulation frequency Ω. R and α represent the dimensionless coupling strengths between the qubit and the dissipative and dephasing reservoirs, respectively.

where $\zeta(t) = \langle g \left| \rho_{\mathrm{q}}(t) \right| e \rangle$, i.e., the off-diagonal element of $\rho_{\mathrm{q}}(t)$), corresponds to the well-known l_1-norm of coherence [16, 17], and $P_g(t) = \langle g \left| \rho_q(t) \right| g \rangle$ represents the population of the qubit ground state. These time-dependent elements of the qubit density matrix are given by [82]

$$
\begin{aligned}
\zeta(t) &= \zeta(0) e^{i\tilde{\omega}(t) - \Gamma(t)/2 - \tilde{\Gamma}(t)}, \\
P_g(t) &= e^{-\Gamma(t)}[P_g(0) + G(t)],
\end{aligned} \tag{8}
$$

where

$$
\begin{aligned}
\Gamma(t) &= \frac{1}{2}\int_0^t dt' (\gamma_1(t') + \gamma_2(t')), \\
\tilde{\Gamma}(t) &= \int_0^t dt' \gamma_3(t'), \\
\tilde{\omega}(t) &= \int_0^t dt' \omega(t'), \\
G(t) &= \frac{1}{2}\int_0^t dt' e^{\Gamma(t')} \gamma_1(t').
\end{aligned} \tag{9}
$$

To capture the dynamics of the system, it is necessary to find the time-dependent functions in Equation (9), which are associated with the time-dependent rates of the master equation. To achieve this, we employ an intuitive heuristic model that ensures complete positivity and trace preservation (CPTP) [82], the formal proofs of which are provided in Appendix B. In this approach, the decay rates are first determined for the zero-temperature case, which are then extended to the nonzero-temperature scenario.

In the following, we first consider a thermal dissipative reservoir and successively include a second thermal pure-dephasing reservoir.

3 | Driven Qubit in a Thermal Dissipative Reservoir

We first consider the case where the qubit interacts only with a dissipative reservoir. Therefore, the rate associated with pure-dephasing is zero, i.e., $\gamma_3(t) = 0$ in the master equation of Equation (5). As discussed above, we begin with the scenario of a zero-temperature ($T_1 = 0$) dissipative reservoir, which further implies $\gamma_2(t) = 0$ in Equation (5). From the Hamiltonian perspective, these conditions allow us to omit H_{r2} and $H_{\mathrm{I,deph}}$ in Equation (1). Under these assumptions, the aim is to derive the expression for the decay rate $\gamma_1(t)$.

With the simplifications above, we can obtain the effective Hamiltonian in the interaction picture via $H_{\mathrm{eff}} = U_0^\dagger H U_0 + i(\partial U_0^\dagger / \partial t) U_0$, where the unitary transformation is given by [61]

$$
U_0 = \exp\left[-i \left\{ \sum_k \omega_k a_k^\dagger a_k t + [\omega_0 t + (\delta/\Omega)\sin(\Omega t)]\sigma_z/2 \right\} \right]. \tag{10}
$$

Using this transformation, the effective Hamiltonian becomes

$$
\begin{aligned}
H_{\mathrm{eff}} &= \sum_k g_k \sigma_+ a_k e^{-i(\omega_k - \omega_0)t} e^{i(\delta/\Omega)\sin(\Omega t)} \\
&\quad + \sum_k g_k^* a_k^\dagger \sigma_- e^{i(\omega_k - \omega_0)t} e^{-i(\delta/\Omega)\sin(\Omega t)}.
\end{aligned} \tag{11}
$$

the formal proof is presented in Appendix A.2.

Using the Jacobi–Anger expansion, the exponential factors in Equation (11) can be written as

$$
e^{\pm i(\delta/\Omega)\sin(\Omega t)} = J_0\left(\frac{\delta}{\Omega}\right) + 2\sum_{n=1}^{\infty} (\pm i)^n J_n\left(\frac{\delta}{\Omega}\right)\cos(n\Omega t), \tag{12}
$$

where $J_n\left(\frac{\delta}{\Omega}\right)$ is the n-th Bessel function of the first kind.

A zero-temperature reservoir implies that at most one excitation exists due to the spontaneous emission of the qubit. Consequently, the combined state of the qubit and the reservoir can be expressed as $|\Psi(0)\rangle = \frac{1}{\sqrt{2}}(|e\rangle + |g\rangle)\,|0\rangle$, where $|0\rangle$ is the vacuum state of the reservoir. The conservation of the total number of excitations leads to the time-evolved state of the system $|\Psi(t)\rangle = \frac{1}{\sqrt{2}}C(t)|e\rangle|0\rangle + \frac{1}{\sqrt{2}}|g\rangle|0\rangle + \sum_k C_k(t)|g\rangle|1_k\rangle$, where $|1_k\rangle$ describes the presence of a single photon in mode k of the reservoir, and

$C_k(t)$ represents the corresponding probability amplitude. Solving the time-dependent Schrödinger equation for the total system yields the differential equation for the probability amplitude $C(t)$, given by

$$\dot{C}(t) + \int_0^t dt' F(t,t') C(t') = 0, \tag{13}$$

where the correlation function $F(t,t')$ can be expressed in terms of the continuous spectrum of the environment frequencies, as detailed in Ref. [61], as

$$F(t,t') = \exp[i(\delta/\Omega)\{\sin(\Omega t) - \sin(\Omega t')\}] \times \int_0^\infty J(\omega) e^{-i(\omega-\omega_0)(t-t')} d\omega, \tag{14}$$

where $J(\omega)$ is the spectral density of the reservoir. We assume that the spectral density of the dissipative reservoir follows a Lorentzian profile [44, 47], given by

$$J(\omega) = \frac{1}{2\pi} \frac{\gamma\lambda^2}{[(\omega_0 - \omega)^2 + \lambda^2]}, \tag{15}$$

where λ represents the spectral width of the coupling, and γ denotes the spontaneous emission decay rate [48]. For the analysis, we can introduce the dimensionless parameter $R = \gamma/\lambda$ which quantifies the coupling strength between the driven qubit and the dissipative reservoir (see Figure 1): $R < 1$ means a weak coupling regime, while $R > 1$ indicates a strong coupling regime.

Strictly speaking, the Fourier transform of the Lorentzian spectrum over the interval $[0, \infty)$, in Equation (14), differs from the full-line transform over $(-\infty, +\infty)$. However, for the physical regime considered here, where the Lorentzian spectral density in Equation (15) is centered at ω_0 with spectral width $\lambda \ll \omega_0$ (i.e., a narrow distribution centered far from the origin), the contribution from negative frequencies becomes negligibly small:

$$\begin{aligned}\int_{-\infty}^0 d\omega\, J(\omega) &= \frac{\gamma\lambda^2}{2\pi} \int_{-\infty}^0 \frac{d\omega}{(\omega_0 - \omega)^2 + \lambda^2} \\ &\approx \frac{\gamma\lambda^2}{2\pi} \frac{[\arctan(-\omega_0/\lambda) + \pi/2]}{\lambda} \\ &\approx \frac{\gamma\lambda}{2\pi} e^{-2\omega_0/\lambda} \ll \frac{\gamma}{2}.\end{aligned} \tag{16}$$

This approximation is well established in the theory of non-Markovian decay in structured reservoirs [83, 84] and in the quasimode theory of quantum optical processes [85]. The condition $\lambda \ll \omega_0$ is physically well motivated for optical and superconducting qubit systems, where the qubit transition frequency is typically several orders of magnitude larger than the reservoir bandwidth.

With the Lorentzian spectral density of Equation (15), one obtains an explicit expression for the correlation function as $F(t,t') = \frac{\gamma\lambda}{2} e^{-\lambda(t-t')} e^{i(\delta/\Omega)(\sin(\Omega t) - \sin(\Omega t'))}$, which substituted in Equation (13) gives [61]

$$\dot{C}(t) = -\frac{\gamma\lambda}{2} e^{i(\delta/\Omega)\sin(\Omega t)} \times \int_0^t dt'\, e^{-i(\delta/\Omega)\sin(\Omega t')} e^{-\lambda(t-t')} C(t'). \tag{17}$$

The solution of the above equation for the probability amplitude $C(t)$ is used to obtain the quantum coherence $\zeta(t)$ of the qubit interacting with a zero-temperature dissipative reservoir, as reported in Ref. [61].

After recalling the result for the zero-temperature case, we now extend the analysis to nonzero temperatures by relating the probability amplitude $C(t)$ to the decay rates $\gamma_1(t)$ and $\gamma_2(t)$ in the master equation of Equation (5). The reservoir at a finite temperature T_1 introduces thermal effects, described by the Bose–Einstein mean occupation number, $\bar{n} = (e^{(\hbar\omega/K_B T_1)} - 1)^{-1}$. Here, K_B represents Boltzmann's constant [86], and $\omega_T = K_B T_1/\hbar$ defines the thermal frequency [87]. The decay rates incorporating the effects of nonzero temperatures are given by $\gamma_1(t)/2 = (\bar{n} + 1) f(t)$ and $\gamma_2(t)/2 = \bar{n} f(t)$ [82], where $f(t)$ is

$$f(t) = -2\mathrm{Re}\left(\frac{\dot{C}(t)}{C(t)}\right). \tag{18}$$

The time-dependent decay rate $\Gamma(t)$ is analytically calculated by substituting the above expression in Equation (9), that is

$$\Gamma(t) = -\ln\left|\frac{C(t)}{C(0)}\right|^{2\bar{n}+1}. \tag{19}$$

Thanks to these expressions, from Equations (8) and (9) we obtain the quantum coherence $\zeta(t)$ and the population of ground state $P_g(t)$ as

$$\begin{aligned}\zeta(t) &= \zeta(0)\left|\frac{C(t)}{C(0)}\right|^{2\bar{n}+1} \\ P_g(t) &= P_g(0)\left|\frac{C(t)}{C(0)}\right|^{2(2\bar{n}+1)} + \frac{\bar{n}+1}{2\bar{n}+1}\left(1 - \left|\frac{C(t)}{C(0)}\right|^{2(2\bar{n}+1)}\right).\end{aligned} \tag{20}$$

Using Equation (20), we can now numerically compute the time behavior of qubit coherence and population, under different temperature regimes and frequency modulation settings.

As a first result, Figure 2 shows the time behavior of coherence $\zeta(t)$ and excited state population $P_e(t) = 1 - P_g(t)$ as functions of the scaled (dimensionless) time γt. We take the qubit in a strong coupling regime $R = 100$ with a low-temperature reservoir ($K_B T_1 = 2.6 \times 10^{-3} \hbar\omega_0$). Figure 2 compares two scenarios: a driven qubit with optimal modulation parameters [61] $\delta = 2.40483\Omega$, $\Omega = 5\gamma$ (dotted red lines) and a qubit without external driving ($\delta = 0, \Omega = 0$; solid blue lines). Notice that the optimal modulation parameters are those which enable the most effective endurance of quantumness. The plots in Figure 2 demonstrate that frequency modulation (FM) significantly extends both the coherence and the excited-state population compared to the undriven case. In particular, at $\gamma t = 1000$, the frequency-modulated qubit retains a coherence value of $\zeta(t) \approx 0.816$ (see the

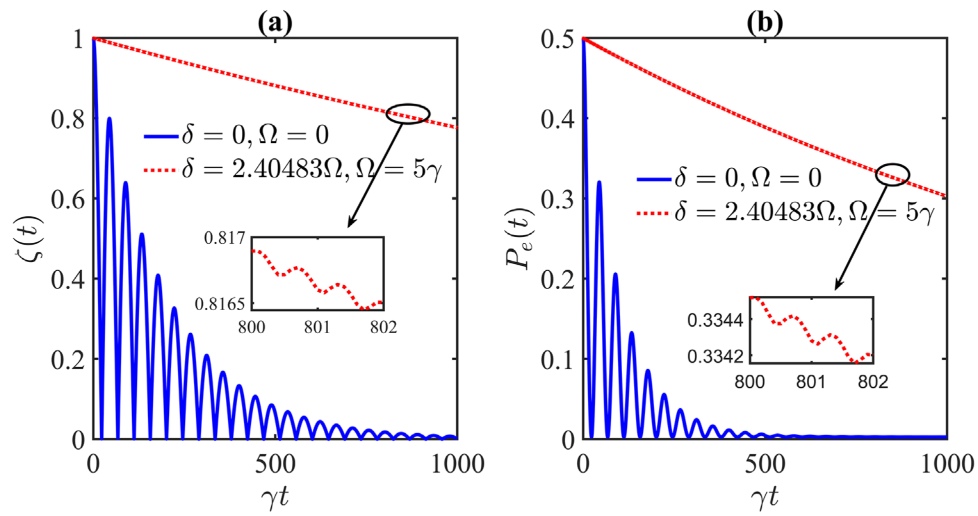

FIGURE 2 | (a) Qubit coherence $\zeta(t)$ and (b) excited state population $P_e(t)$ as functions of scaled dimensionless time γt under a low-temperature reservoir with $K_B T_1 = 2.6 \times 10^{-3} \hbar\omega_0$. The results are shown for optimal amplitude and frequency modulations with $\delta = 2.40483\Omega$, $\Omega = 5\gamma$ (dotted red line), and for the case of no driving field $\Omega = 0$ (solid blue line). The qubit is in the strong coupling regime with $R = 100$.

inset of Figure 2a), whereas the undriven qubit has completely decohered, yielding $\zeta(t) \approx 0$. The coherence time, defined as the time at which $\zeta(t)$ decays to $1/e$ of its initial value, increases from $t_c \approx 2/\gamma$ in the absence of driving to $t_c > 1000/\gamma$ under optimal FM conditions, corresponding to an enhancement factor greater than 500×.

In particular, the coherence dynamics exhibit pronounced non-monotonic behavior over time. Although such non-monotonicity already appears in the undriven system due to the strong system-environment coupling.

To characterize the underlying non-monotonic behavior more precisely, we analyze the rate of change of the quantum coherence measure $C(\rho(t))$, where $\zeta(t)$ serves as the corresponding coherence indicator [88, 89]. For a strictly Markovian evolution, the time derivative of any contractive state measure remains monotonically non-positive,

$$\frac{d}{dt} C(\rho(t)) \leq 0, \tag{21}$$

reflecting the continuous and irreversible loss of information from the qubit to its surrounding environment. Conversely, the temporary violations of this monotonic behavior observed in Figure 2, namely intervals where

$$\frac{d}{dt} C(\rho(t)) > 0, \tag{22}$$

provide a clear mathematical witness of non-Markovianity. Physically, these positive derivatives correspond to the revivals and fluctuations visible in the coherence dynamics, indicating a temporary backflow of information from the structured environmental fields into the open quantum system.

The non-monotonic behavior of coherence in the dotted red lines of Figure 2 can be associated with non-Markovian effects in the system dynamics, which are also present in the case without driving due to the chosen strong-coupling conditions.

We then place the qubit in reservoirs at intermediate temperature ($K_B T_1 = 2.6\hbar\omega_0$) and high temperature ($K_B T_1 = 260\hbar\omega_0$). The plots of coherence $\zeta(t)$ and excited state population $P_e(t)$ as functions of scaled time are reported in Figures 3 and 4, respectively. As done before, Figures 3 and 4 show the case without driving field ($\delta = 0, \Omega = 0$) the case with the action of a driving field under optimal modulation parameters (same as before). Again, optimal FM allow a preservation of quantum coherence and excited state population much longer than the case without control, as illustrated by the dotted red lines in Figures 3. Specifically, at $\gamma t = 400$, the frequency-modulated qubit maintains coherence at $\zeta(t) \approx 0.646$ (see Figure 3a), whereas the undriven case undergoes complete decoherence within $\gamma t \approx 50$. The resulting enhancement factor in coherence time exceeds 8×. The observed fluctuations in both coherence and population provide a clear signature of non-Markovian dynamics in the system.

Even at $K_B T_1 = 260\hbar\omega_0$, frequency modulation (FM) maintains coherence up to $\gamma t \approx 40$ (dotted red line in Figure 4a), compared to the quick decoherence ($\gamma t \lesssim 1$) in the absence of driving (solid blue line). While the absolute coherence values are significantly reduced due to strong thermal effects, FM still provides a substantial relative advantage, extending the coherence time by a factor of ~ 40× compared to the undriven case. The rapid initial decay reflects strong thermal dissipation, whereas the subsequent plateau highlights the protective effect of FM even in extreme temperature regimes.

These results prove that the technique of FM of the qubit effectively mitigates the dissipative effects of temperature, even in the high-temperature regime.

4 | Driven Qubit Under Independent Thermal Dissipative and Dephasing Noises

In this section, we consider a single qubit interacting with a thermal phase-covariant reservoir, made of two types of environmental noise to better approximate real-world conditions:

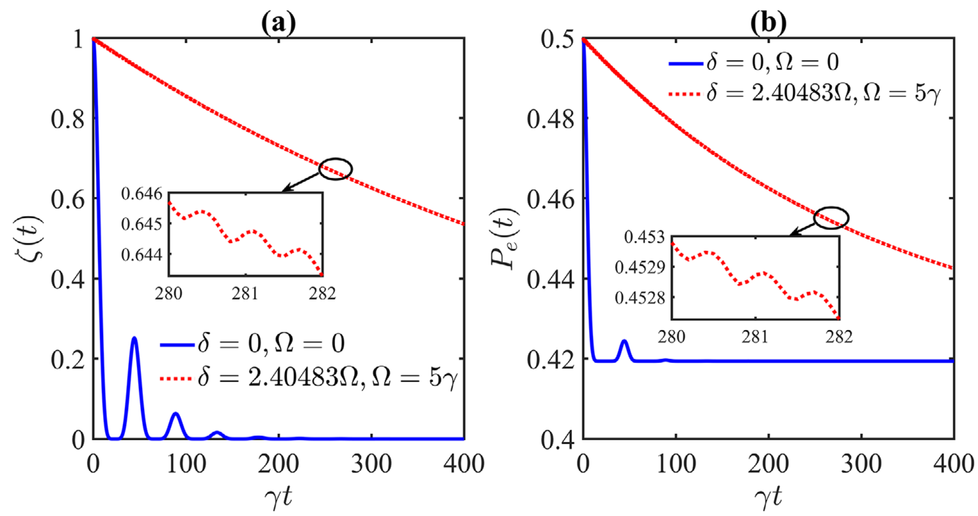

FIGURE 3 | (a) Qubit coherence $\zeta(t)$ and (b) excited state population $P_e(t)$ as functions of the scaled time γt under an intermediate-temperature reservoir with $K_B T_1 = 2.6\hbar\omega_0$. The results are shown for optimal amplitude and frequency modulations with $\delta = 2.40483\Omega$, $\Omega = 5\gamma$ (dotted red line), and for the case of no driving field $\Omega = 0$ (solid blue line). The qubit is in the strong coupling regime with $R = 100$.

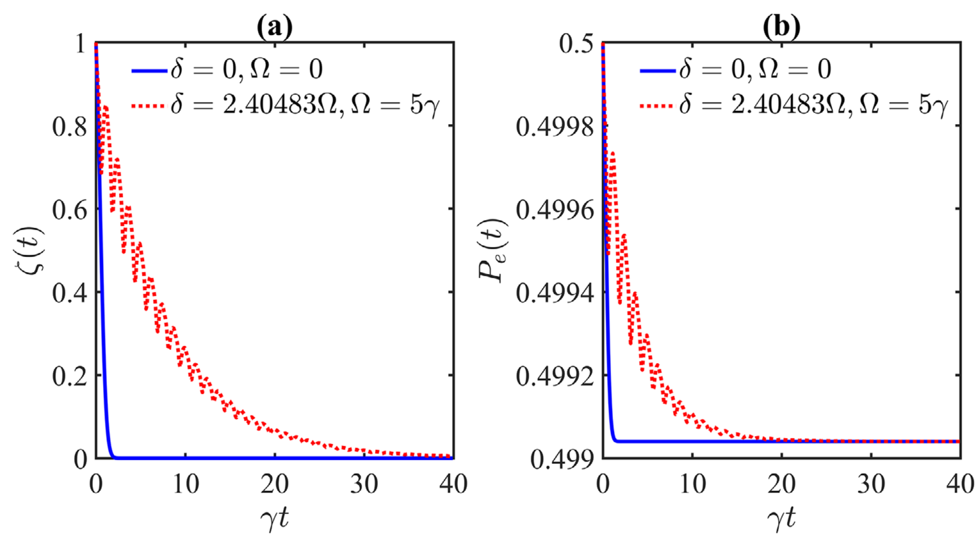

FIGURE 4 | (a) Qubit coherence $\zeta(t)$ and (b) excited state population $P_e(t)$ as functions of scaled time γt under a high-temperature reservoir with $K_B T_1 = 260\hbar\omega_0$. The results are shown for optimal amplitude and frequency modulations with $\delta = 2.40483\Omega$, $\Omega = 5\gamma$ (dotted red line), and for the case of no driving field $\Omega = 0$ (solid blue line). The qubit is in the strong coupling regime with $R = 100$.

dissipative noise at temperature T_1 and pure-dephasing noise at temperature T_2.

We begin by only considering a pure-dephasing noise to simplify the analysis. This assumption sets the rates $\gamma_1(t) = \gamma_2(t) = 0$ in the master equation of Equation (5). Under these conditions, H_{r1} and $H_{\mathrm{I,dis}}$ are neglected. The effective Hamiltonian in the interaction picture $H'_{\mathrm{eff}} = U_0^\dagger H U_0 + i(\partial U_0^\dagger/\partial t)U_0$, with the unitary evolution operator from Equation (10), is given by

$$H'_{\mathrm{eff}} = \sigma_z \sum_l \left(f_l b_l^\dagger e^{i\mu_l t} + f_l^* b_l e^{-i\mu_l t} \right). \tag{23}$$

the formal proof is presented in Appendix A.3. As is evident from the above equation, FM does not affect the system evolution because the interaction Hamiltonian $H_{\mathrm{I,deph}}$ of Equation (4) commutes with the free Hamiltonian of the qubit H_{q} of Equation (2). This is an important observation, as it shows that FM is completely ineffective in decoupling the qubit from the dephasing environment. Before studying the role of both dissipative and dephasing noise at given temperature, it is useful to briefly review the exact dynamics of the qubit interacting with a pure-dephasing reservoir [90].

The effective Hamiltonian in Equation (23) permits to derive the time-evolution operator for the qubit and the pure-dephasing reservoir as [90]

$$U(t) = \exp\left[\frac{\sigma_z}{2} \sum_l \left(b_l^\dagger \xi_l(t) - b_l \xi_l^*(t) \right) \right], \tag{24}$$

where $\xi_l(t) = 2f_l(1 - e^{i\mu_l t})/\mu_l$. For clarity and without loss of generality, let us consider the qubit at $t = 0$ interacting with a zero-temperature pure-dephasing reservoir. The initial state of the system is given as $|\psi(0)\rangle = (c_1 |e\rangle + c_2 |g\rangle) |0_l\rangle$, where $|0_l\rangle$ represents the vacuum state of the field mode l. Consequently, the evolved state of both qubit and reservoir is $|\psi(t)\rangle = c_1 |e\rangle |\frac{1}{2}\xi_l(t)\rangle + c_2 |g\rangle |-\frac{1}{2}\xi_l(t)\rangle$, where $|\frac{1}{2}\xi_l(t)\rangle$ is a coherent state with amplitude $\frac{1}{2}\xi_l(t)$. Tracing over the reservoir modes reveals that the populations remain unaffected, while the off-diagonal elements of the qubit density matrix, ruled by $\zeta(t) = \zeta(0)e^{-\tilde{\Gamma}(t)}$, decay over time. This decay arises due to the diminishing overlap between the different field states associated with the qubit evolution [90].

In a more general scenario where the reservoir is at a finite temperature ($T_2 > 0$), the time dependent decay rate $\gamma_3(t)$ and dephasing factor $\tilde{\Gamma}(t)$ become [82, 91]

$$\gamma_3(t) = \int_0^\infty d\omega J(\omega) \coth(\hbar\omega/2k_B T_2) \frac{\sin(\omega t)}{\omega}, \quad (25)$$

$$\tilde{\Gamma}(t) = 2\int_0^\infty d\omega J(\omega) \coth(\hbar\omega/2k_B T_2) \frac{1 - \cos(\omega t)}{\omega^2}, \quad (26)$$

where $J(\omega)$ is the spectral density. Here, we assume that the dephasing reservoir has an Ohmic spectral density [44], given by

$$J(\omega) = \alpha\omega^s e^{-\omega/\omega_c}, \quad (27)$$

characterized by a cutoff frequency ω_c that depends on the particular physical system under consideration and ensures that $J(\omega) \to 0$ for $\omega \gg \omega_c$ [87]. In this context, $\alpha > 0$ is a dimensionless constant that defines the strength of the system-bath coupling (see Figure 1), while s denotes the dimensionality of the field. By changing the parameter s, one can transition from sub-Ohmic reservoirs ($s < 1$) to Ohmic reservoirs ($s = 1$) and super-Ohmic reservoirs ($s > 1$), respectively. In our analysis we focus on the one-dimensional field scenario ($s = 1$). Substituting Equation (25) into Equation (9) allows us to get the quantum coherence $\zeta(t)$ of Equation (8) for the thermal pure-dephasing reservoir.

We now switch on both noises, dissipative and dephasing, at the same time. Using the additivity property of coherence decay rates [78], the relaxation rate of a system subjected to multiple weak noise sources is equal to the sum of the relaxation rates corresponding to each individual noise source, that is $\gamma_{\text{tot}} = \frac{\gamma_1(t)}{2} + \frac{\gamma_2(t)}{2} + \gamma_3(t)$. Therefore, the time-dependent quantum coherence in this general scenario can be obtained by multiplying the coherence functions found above for the dissipative and pure-dephasing dynamics separately.

For a Ohmic spectral density of the kind given in Equation (27), it is known that backflow of information and recoherence occur when $s > 2$ [91]. More general decoherence–recoherence events, due to the interplay between Ohmicity paramater and information backflows, can also appear in local dephasing channels by preparing the overall system in suited initial conditions [92–94]. Concerning our analysis, we recall that FM cannot decouple the

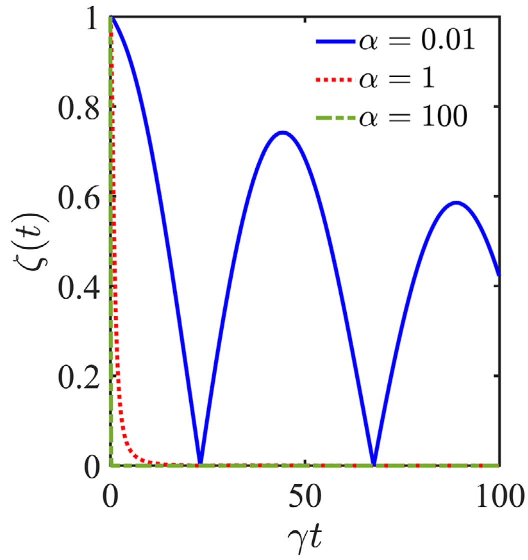

FIGURE 5 | Qubit coherence $\zeta(t)$ as a function of scaled time γt for different values of the dephasing coupling α. The values of other parameters are: $R = 100$, $\delta = 0$, $\Omega = 0$. Both dissipative and dephasing reservoirs are set to zero temperature ($T_1 = T_2 = 0$).

qubit from the dephasing reservoir and the system operates in the Markovian regime for the one-dimensional field scenario ($s = 1$), when only dephasing acts. So, the value of the dephasing coupling α is expected to be very relevant on the possibility of maintaining quantum coherence within the qubit, when analyzing the evolution of coherence under both noises across a range of temperatures.

The above consideration leads us to first fix the temperatures of the reservoirs equal to zero and exclude control effects from the analysis, in order to identify a typical value of α which is not very detrimental for qubit coherence when time goes by. Moreover, we choose $R = 100$ for the dissipative environment, so to have strong coupling and non-Markovian dynamics stemming from system-environment excitation exchange (as noticed in Section 3). From Figure 5, we observe that weak coupling strengths with the dephasing reservoir, of the order of $\alpha = 0.01$, are already enough to permit coherence to last orders of magnitudes longer than the case of stronger couplings.

Therefore, we set $\alpha = 0.01$ and $R = 100$ to numerically study the time behavior of qubit coherence at different temperature regimes. Figure 6 presents the evolution of coherence $\zeta(t)$ as a function of the scaled time γt, for a qubit experiencing a range of temperatures going from low to high values. As done for Figures 2–4, here we compare the results for a driven qubit with optimal modulation parameters ($\delta = 2.40483\Omega$ and $\Omega = 5\gamma$, dotted red lines) and those for a qubit without control ($\delta = 0$ and $\Omega = 0$, solid blue lines).

From Figure 6, we clearly see that applying FM to the qubit preserves coherence for a much longer time compared to the case without control. Importantly, coherence fluctuates well above zero during its evolution for the suitably frequency-modulated qubit (dotted red lines), so avoiding the zeros occurring during the oscillations in the case without control (blue solid lines).

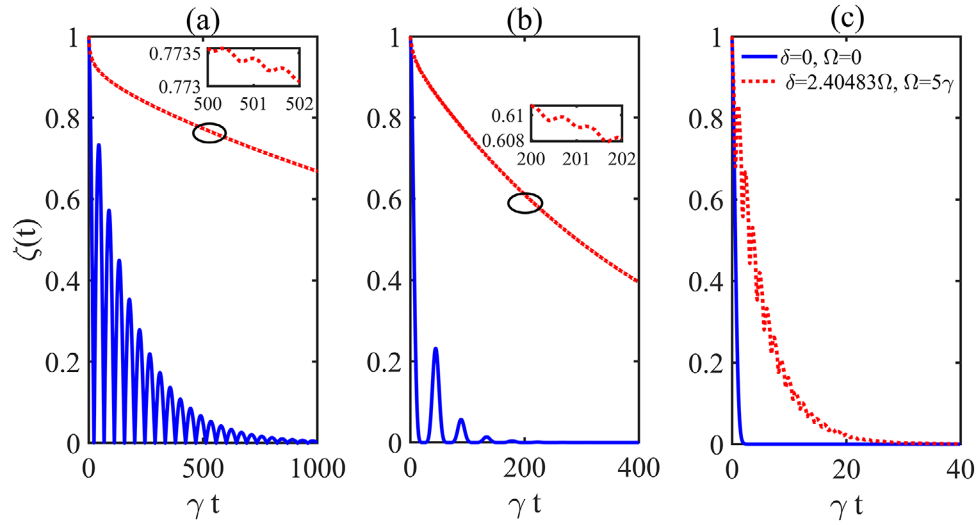

FIGURE 6 | Qubit coherence $\zeta(t)$ as a function of scaled time γt for different temperature regimes: (a) $K_BT_1 = 2.6\times10^{-3}\hbar\omega_0$, $K_BT_2 = 10^{-5}\hbar\omega_c$, (b) $K_BT_1 = 2.6\hbar\omega_0$, $K_BT_2 = 10^{-2}\hbar\omega_c$, (c) $K_BT_1 = 2.6\times10^{2}\hbar\omega_0$, $K_BT_2 = \hbar\omega_c$. The results are shown for optimal amplitude and frequency modulations with $\delta = 2.40483\Omega$, $\Omega = 5\gamma$ (dotted red line), and no driving $\Omega = 0$ (solid blue line). The qubit is in the weak coupling regime with the pure-dephasing reservoir ($\alpha = 0.01$) and in the strong coupling regime with the dissipative reservoir ($R = 100$).

Fluctuations indicate a signature of non-Markovianity in the qubit, which is present even in the high-temperature regime due to the interplay between FM and strong coupling with the dissipative noise. The results indicate that FM has the capability to efficiently preserve quantum coherence within the qubit when the dephasing coupling α is sufficiently small (of the order of 0.01).

An interesting question now arises: what is the threshold value α_{th} of the dephasing coupling beyond which the enhancement effect due to qubit FM no longer occurs, such that coherence evolves equally for a controlled and uncontrolled qubit?

To address this question, the threshold value α_{th} in our simulations is defined as the value of α at which, when plotting the coherence as a function of time for the two cases, namely without modulation ($d = 0$) and with modulation ($d = 2.40483\,\Omega$), their coherence times become equal.

In Markovian open quantum systems, the coherence time t_c is defined as the time when $\zeta(t_c) = \zeta(0)/e$, i.e.,

$$t_c = \frac{1}{\gamma}. \tag{28}$$

However, for a non-Markovian system, this simple exponential model does not hold, and defining the coherence time is more challenging. Due to the non-Markovian nature of the dynamics, coherence plots exhibit fluctuations. To overcome this, we extract the envelope of each oscillating curve, which mimics the monotonic decay characteristic of Markovian behavior. Using this envelope, we can define the coherence time in a way consistent with the Markovian approach described above.

Applying this definition, at very low temperature (case of Figure 6a) we obtain $\alpha_{\text{th}} = 0.75$. Consequently, FM-based quantumness enhancement at low temperature occurs when $\alpha \le 0.75$. At intermediate temperature (case of Figure 6b), we find $\alpha_{\text{th}} = 0.6$. Furthermore, our numerical analysis establishes that α_{th} decreases monotonically as temperature increases, reaching its minimum value of 0.45 in the infinite-temperature limit (case of Figure 6c). Determining these thresholds is crucial because they identify the boundaries where FM ceases to be effective to genuinely enhance coherence. They serve as design guidelines for optimizing control parameters Γ and δ, ensuring that resources are used efficiently.

5 | Conclusion

In this work, we have explored the impact of frequency modulation (FM) as a control technique for preserving quantum coherence in a thermally noisy system by mitigating the detrimental effects of temperature. Through a systematic analysis of coherence dynamics and relevant time scales, we have established three main conclusions.

First, FM is highly effective in counteracting thermal dissipation. It significantly extends coherence times in dissipative thermal reservoirs, with enhancement factors exceeding 500× at low temperatures ($K_BT_1 = 2.6\times10^{-3}\hbar\omega_0$). Remarkably, this protection remains substantial even in the high-temperature regime ($K_BT_1 = 260\hbar\omega_0$), where coherence times are still extended by factors of $\sim 40\times$. This improvement originates from a dynamical decoupling mechanism induced by the time-dependent modulation, which effectively detunes the qubit from the dominant thermal noise spectrum.

Second, we identify a fundamental limitation of FM under pure dephasing noise. Due to the commutation relation $[H_q, H_{I,\text{deph}}] = 0$ between the qubit self-Hamiltonian and the dephasing interaction Hamiltonian, the applied modulation cannot alter the dephasing dynamics. As a result, FM remains ineffective against pure dephasing regardless of control parameters. This highlights an intrinsic constraint of FM-based protection strategies that must be accounted for in realistic implementations.

Third, in the presence of both dissipative and dephasing noise channels, FM exhibits a clear threshold behavior. Effective protection is achieved only when the dephasing coupling strength α remains below a temperature-dependent critical value,

$$\alpha_{\rm th} = 0.75 \quad \text{(low temperature)},$$

$$\alpha_{\rm th} = 0.60 \quad \text{(intermediate temperature)},$$

$$\alpha_{\rm th} = 0.45 \quad \text{(high temperature limit)}.$$

These thresholds decrease monotonically with increasing temperature, indicating that thermal effects in the dephasing environment progressively suppress the benefit of FM. When $\alpha > \alpha_{\rm th}$, dephasing noise dominates and FM provides no improvement over the undriven dynamics.

These results suggest several promising avenues for further investigation. One natural extension is the exploration of optimized non-sinusoidal modulation protocols, such as piecewise-constant or numerically optimized control pulses, which may overcome limitations inherent to harmonic driving. Another important direction is the development of hybrid schemes combining FM with dynamical decoupling or quantum error correction, potentially enabling simultaneous protection against both dissipative and dephasing noise. Experimental validation in platforms such as superconducting quantum circuits with Josephson junctions [60, 95–98] and semiconductor artificial atoms [99] would be essential to assess practical feasibility. Finally, extending this framework to multi-qubit architectures and entanglement preservation in quantum networks [76, 77] represents a natural step toward quantum information processing applications.

Overall, frequency modulation provides a simple yet effective mechanism for mitigating decoherence in thermal environments, provided that its intrinsic limitations are properly understood and operational parameters are chosen within the regime where protection is effective.

Acknowledgements

R.L.F. acknowledges support by MUR (Ministero dell'Università e della Ricerca) through the following projects: PNRR Project ICON-Q – Partenariato Esteso NQSTI – PE00000023 – Spoke 2 – CUP: J13C22000680006, PNRR Project QUANTIP – Partenariato Esteso NQSTI – PE00000023 – Spoke 9 – CUP: E63C22002180006. R.M. acknowledges support from the Canada Research Chair program, as well as from NSERC, through the following projects: AQUA ALLRP 587602-23, QuEnSi ALLRP 578468-22, Consortium on Integrated Quantum Photonics with Ferroelectric Materials ALLRP 587352-23, HyperSpace ALLRP 569583-21, and from FRQNT, through the project AdéQuATS FRQNT 328872.

Open access publishing facilitated by Universita degli Studi di Palermo, as part of the Wiley - CRUI-CARE agreement.

Conflicts of Interest

The author declare no conflicts of interest.

Data Availability Statement

Data sharing not applicable to this article as no datasets were generated or analyzed during the current study.

Appendix A: Derivation of the Time-Local Master Equation

In this Appendix, we provide the detailed derivation of the time-local master Equation (5) starting from the total Hamiltonian given in Equation (1). We explicitly perform the trace over the thermal reservoirs and show the emergence of the Lindblad-type structure with time-dependent decay rates.

A.1 | Interaction Picture Transformation

The total Hamiltonian is given by

$$H = H_q + H_{r1} + H_{r2} + H_{I,\rm dis} + H_{I,\rm deph}, \tag{A.1}$$

where the FM-driven qubit Hamiltonian reads

$$H_q = \frac{\hbar}{2}(\omega_0 + \delta\cos(\Omega t))\sigma_z. \tag{A.2}$$

We move to the interaction picture using the unitary operator (Equation (10)):

$$U_0(t) = \exp\left[-i\left(\sum_k \omega_k a_k^\dagger a_k t + \frac{1}{2}\left(\omega_0 t + \frac{\delta}{\Omega}\sin(\Omega t)\right)\sigma_z\right)\right]. \tag{A.3}$$

The interaction-picture Hamiltonian is defined as

$$H_{\rm int}(t) = U_0^\dagger(t) H U_0(t) + i\left(\partial_t U_0^\dagger(t)\right)U_0(t), \tag{A.4}$$

so,

$$\begin{aligned} H_{\rm int}(t) &= U_0^\dagger(t)(H_{I,\rm dis} + H_{I,\rm deph})U_0(t) \\ &\quad + U_0^\dagger(t)(H_q + H_{r1} + H_{r2})U_0(t) + i\left(\partial_t U_0^\dagger(t)\right)U_0(t). \end{aligned} \tag{A.5}$$

A.2 | Dissipative Interaction

When the qubit interacts only with a dissipative reservoir, the interaction-picture Hamiltonian is defined as

$$\begin{aligned} H_{\rm int}(t) &= U_0^\dagger(t)\, H_{I,\rm dis}\, U_0(t) \\ &\quad + U_0^\dagger(t)(H_q + H_{r1})U_0(t) + i\left(\partial_t U_0^\dagger(t)\right)U_0(t). \end{aligned} \tag{A.6}$$

To obtain Equation (11) explicitly, we apply the unitary transformation $U_0(t)$ to the interaction Hamiltonian $H_{I,\rm dis} = \sum_k \left(g_k\sigma_+ a_k + g_k^* a_k^\dagger \sigma_-\right)$.

The first term in the transformation yields

$$U_0^\dagger \sigma_+ U_0 = \sigma_+ \exp\left\{i\left[\omega_0 t + \left(\frac{\delta}{\Omega}\right)\sin(\Omega t)\right]\right\}. \tag{A.7}$$

This result follows from the Baker–Campbell–Hausdorff expansion together with the commutation relation

$$[\sigma_z, \sigma_+] = 2\sigma_+. \tag{A.8}$$

Similarly, for the reservoir operators,

$$U_0^\dagger a_k U_0 = a_k e^{-i\omega_k t}, \tag{A.9}$$

since

$$[a_k^\dagger a_k, a_k] = -a_k. \tag{A.10}$$

Combining these transformations, we obtain

$$U_0^\dagger (g_k \sigma_+ a_k) U_0 = g_k \sigma_+ a_k \exp\left[-i(\omega_k - \omega_0)t\right] \times \exp\left[i\left(\frac{\delta}{\Omega}\right)\sin(\Omega t)\right]. \tag{A.11}$$

The Hermitian conjugate term follows analogously. The Jacobi–Anger expansion in Equation (12) then decomposes the modulation factor

$$\exp\left[i\left(\frac{\delta}{\Omega}\right)\sin(\Omega t)\right] \tag{A.12}$$

into a series of sidebands at frequencies $\pm n\Omega$, thereby enabling the analysis of multi-photon processes induced by the frequency modulation.

The Hermitian conjugate term follows similarly. The resulting effective Hamiltonian as the interaction-picture Hamiltonian, is

$$H_{\text{eff}}(t) = \sum_k g_k \sigma_+ a_k e^{-i(\omega_k - \omega_0)t} e^{i\frac{\delta}{\Omega}\sin(\Omega t)} + \text{H.c.} \tag{A.13}$$

A.3 | Dephasing Interaction

When the qubit interacts only with a pure-dephasing reservoir, we have

$$H_{\text{int}}(t) = U_0^\dagger(t) H_{I,\text{diph}}\, U_0(t) + U_0^\dagger(t)\left(H_q + H_{r2}\right)U_0(t) + i\left(\partial_t U_0^\dagger(t)\right)U_0(t). \tag{A.14}$$

$$H_{I,\text{deph}} = \sum_l \sigma_z \left(f_l b_l + f_l^* b_l^\dagger\right), \tag{A.15}$$

we note that $[\sigma_z, H_q] = 0$, hence

$$U_0^\dagger \sigma_z U_0 = \sigma_z. \tag{A.16}$$

Therefore,

$$H'_{\text{eff}}(t) = \sigma_z \sum_l \left(f_l b_l e^{-i\mu_l t} + f_l^* b_l^\dagger e^{i\mu_l t}\right). \tag{A.17}$$

Importantly, the modulation does not enter this Hamiltonian, reflecting the fact that $[\sigma_z, \sigma_z] = 0$, which is the origin of FM ineffectiveness against pure dephasing.

A.4 | Reduced Dynamics and Master Equation

We assume an initially factorized state

$$\rho_{\text{tot}}(0) = \rho_q(0) \otimes \rho_{r1} \otimes \rho_{r2}, \tag{A.18}$$

with thermal reservoirs

$$\rho_{ri} = \frac{e^{-\beta_i H_{ri}}}{Z_i}, \qquad \beta_i = \frac{1}{k_B T_i}. \tag{A.19}$$

The reduced density matrix is

$$\rho_q(t) = \text{Tr}_{r1,r2}\left[U(t)\rho_{\text{tot}}(0)U^\dagger(t)\right]. \tag{A.20}$$

Within the second-order Born approximation and a time-convolutionless expansion, the dynamics reads

$$\dot\rho_q(t) = -i[H_q, \rho_q(t)] + \sum_{i=1}^{3} \gamma_i(t)\mathcal{L}_i[\rho_q(t)]. \tag{A.21}$$

Special cases of this master equation include those considered, for instance, in Refs. [100–103] for $\gamma_1(t) = \gamma_3(t) = 0$, which describes an dissipative model, and the pure-dephasing master equation considered in Refs. [91, 102–106] for $\gamma_1(t) = \gamma_2(t) = 0$. These two special cases can be derived using an exact approach starting from a microscopic Hamiltonian model for the system and environment; hence, the resulting dynamics is always completely positive and trace-preserving (CPTP). In the more general case considered in this paper, however, the master equation is introduced phenomenologically, as an exact microscopic derivation is unfeasible. Nevertheless, a diagonalization procedure results in a unique- and in this sense canonical- representation of the equation, which I present in Appendix C.

A.5 | Time-Dependent Decay Rates

The dissipative rates are

$$\frac{\gamma_1(t)}{2} = (\bar n + 1) f(t), \qquad \frac{\gamma_2(t)}{2} = \bar n f(t), \tag{A.22}$$

where $\bar n = \left[e^{\hbar\omega_0/k_B T_1} - 1\right]^{-1}$ and

$$f(t) = -2\,\text{Re}\left[\frac{\dot C(t)}{C(t)}\right]. \tag{A.23}$$

The reservoir correlation function is

$$F(t,t') = e^{i\frac{\delta}{\Omega}(\sin(\Omega t) - \sin(\Omega t'))} \int_0^\infty d\omega\, J(\omega) e^{-i(\omega-\omega_0)(t-t')}. \tag{A.24}$$

The Ohmic dephasing rate is

$$\gamma_3(t) = \int_0^\infty d\omega\, J_{\text{deph}}(\omega) \coth\left(\frac{\hbar\omega}{2k_B T_2}\right)\frac{\sin(\omega t)}{\omega}, \tag{A.25}$$

with $J_{\text{deph}}(\omega) = \alpha\omega e^{-\omega/\omega_c}$.

Appendix B: Complete Positivity

In the following section, we investigate the conditions under which the master equation Equation (5) generates physically dynamics described by a completely positive and trace-preserving (CPTP) map.

Since complete positivity (CP) can be formulated as inequalities involving the Bloch vector components [107], we first express the qubit density operator in the Bloch representation [44, 82, 86, 108]:

$$\rho(0) = \frac{1}{2}(I + \mathbf{v}(0)\cdot\boldsymbol{\sigma}), \tag{B.1}$$

where I is the identity operator, $\boldsymbol{\sigma} = (\sigma_x, \sigma_y, \sigma_z)$ is the vector of Pauli operators, and $\mathbf{v}(0) = (x_1, x_2, x_3)$ is the Bloch vector.

Explicitly, the density matrix reads

$$\rho(0) = \frac{1}{2}\begin{pmatrix} 1 + x_3 & x_1 - ix_2 \\ x_1 + ix_2 & 1 - x_3 \end{pmatrix}. \tag{B.2}$$

The Bloch vector evolves under a linear dynamical map [82, 108]:

$$\Phi : \mathbf{v}(0) \mapsto \mathbf{v}(t) = \Lambda(t)\mathbf{v}(0) + \mathbf{T}(t), \tag{B.3}$$

where the translation vector is

$$\mathbf{T}(t) = (0, 0, t_3(t)), \tag{B.4}$$

and the damping matrix is diagonal,

$$\Lambda(t) = \begin{pmatrix} \lambda_1(t) & 0 & 0 \\ 0 & \lambda_2(t) & 0 \\ 0 & 0 & \lambda_3(t) \end{pmatrix}. \tag{B.5}$$

Here, $\lambda_i(t)$ are the eigenvalues of the dynamical map in the damping basis.

Consequently, the Bloch components evolve as

$$\begin{aligned} x_1(t) &= \lambda_1(t)x_1(0), \\ x_2(t) &= \lambda_2(t)x_2(0), \\ x_3(t) &= \lambda_3(t)x_3(0) + t_3(t). \end{aligned} \tag{B.6}$$

The corresponding density matrix is

$$\rho(t) = \frac{1}{2}(I + \mathbf{v}(t) \cdot \boldsymbol{\sigma}), \tag{B.7}$$

$$\rho(t) = \frac{1}{2}\begin{pmatrix} 1 + \lambda_3(t)x_3 + t_3(t) & \lambda_1(t)x_1 - i\lambda_2(t)x_2 \\ \lambda_1(t)x_1 + i\lambda_2(t)x_2 & 1 - \lambda_3(t)x_3 - t_3(t) \end{pmatrix}. \tag{B.8}$$

By substituting Equation (B.8) into Equation (5), the dynamical parameters take the form

$$\lambda_1(t) = e^{-\Gamma(t)/2 - \tilde{\Gamma}(t) + i\Omega(t)}, \tag{B.9}$$

$$\lambda_2(t) = e^{-\Gamma(t)/2 - \tilde{\Gamma}(t) - i\Omega(t)}, \tag{B.10}$$

$$\lambda_3(t) = e^{-\Gamma(t)}, \tag{B.11}$$

$$t_3(t) = e^{-\Gamma(t)}[1 + 2G(t)] - 1, \tag{B.12}$$

where $\Gamma(t)$, $\tilde{\Gamma}(t)$, $G(t)$, and $\Omega(t)$ are defined in Equation (9).

Using the Choi–Jamiołlkowski isomorphism [109–112], a dynamical map $\rho(t) = \Phi_t(\rho(0))$ is completely positive if and only if the corresponding Choi matrix

$$C = (\Phi_t \otimes I)\big(|\Phi^+\rangle\langle\Phi^+|\big)$$

is completely positive, i.e., $C \geq 0$. Here,

$$|\Phi^+\rangle = \frac{1}{\sqrt{2}}(|00\rangle + |11\rangle). \tag{B.13}$$

The action of the map in the computational basis can be written as

$$\Phi_t(\rho) = \begin{pmatrix} (1-p)\rho_{00} + q\rho_{11} & w\rho_{01} + y\rho_{10} \\ w\rho_{10} + y\rho_{01} & p\rho_{00} + (1-q)\rho_{11} \end{pmatrix}. \tag{B.14}$$

We introduce the combinations

$$p(t) = \frac{1}{2}[t_3(t) + \lambda_3(t)], \qquad q(t) = \frac{1}{2}[t_3(t) - \lambda_3(t)], \tag{B.15}$$

$$w(t) = \frac{1}{2}[\lambda_1(t) + \lambda_2(t)], \qquad y(t) = \frac{1}{2}[\lambda_1(t) - \lambda_2(t)]. \tag{B.16}$$

The resulting Choi matrix has an X-shaped structure [113]:

$$C = \begin{pmatrix} \frac{1}{2} + p & 0 & 0 & w \\ 0 & \frac{1}{2} - p & y & 0 \\ 0 & y & \frac{1}{2} + q & 0 \\ w & 0 & 0 & \frac{1}{2} - q \end{pmatrix}. \tag{B.17}$$

For $C \geq 0$, all eigenvalues must be non-negative. Although direct diagonalization of a 4×4 matrix is generally complicated, the X-shaped allows one to reduce the problem to two independent 2×2 blocks via basis permutation [113]. Reordering the basis as (1,4,2,3) yields

$$C = \begin{pmatrix} \frac{1}{2} + p & w & 0 & 0 \\ w & \frac{1}{2} - q & 0 & 0 \\ 0 & 0 & \frac{1}{2} - p & y \\ 0 & 0 & y & \frac{1}{2} + q \end{pmatrix}, \tag{B.18}$$

which can be written as

$$C = \begin{pmatrix} \frac{1}{2} + p & w \\ w & \frac{1}{2} - q \end{pmatrix} \oplus \begin{pmatrix} \frac{1}{2} - p & y \\ y & \frac{1}{2} + q \end{pmatrix}. \tag{B.19}$$

Therefore, Equation (B.18) is completely positive if and only if [82, 113]

$$|p(t)|, |q(t)| \leq \frac{1}{2}, \tag{B.20}$$

$$w^2(t) \leq \left(\frac{1}{2} + p(t)\right)\left(\frac{1}{2} - q(t)\right), \tag{B.21}$$

and

$$y^2(t) \leq \left(\frac{1}{2} - p(t)\right)\left(\frac{1}{2} + q(t)\right). \tag{B.22}$$

Using the analytical expressions given by Equations (B.9 and 65), the necessary and sufficient conditions for complete positivity (CP) read as follows:

$$\text{i)} \quad 0 \leq e^{-\Gamma(t)}(G(t) + 1) \leq 1, \tag{B.23}$$

$$[1ex]\text{ii)} \quad 0 \leq e^{-\Gamma(t)}G(t) \leq 1, \tag{B.24}$$

$$[1ex]\text{iii)} \quad -e^{-\Gamma(t)-2\tilde{\Gamma}(t)}\sin^2\Omega(t) \le e^{-\Gamma(t)}G(t)\left[1-e^{-\Gamma(t)}(G(t)+1)\right], \tag{B.25}$$

$$[1ex]\text{iv)} \quad e^{-\Gamma(t)-2\tilde{\Gamma}(t)}\cos^2\Omega(t) \le e^{-\Gamma(t)}\left[1-e^{-\Gamma(t)}G(t)\right][G(t)+1]. \tag{B.26}$$

We note that the validity of conditions i)-ii) (the positivity conditions) automatically guarantees that condition iii) is satisfied, since the left-hand side of the inequality is always non-positive, whereas the right-hand side is always non-negative. We also emphasize that the dephasing term described by L_3 directly affects only conditions (iii)–(iv) through the decoherence term $\tilde{\Gamma}(t)$. Finally, we note that the conditions $\Gamma(t) \ge 0$ and $1 \ge G(t) \ge 0$ are sufficient to ensure positivity, namely conditions (i)–(ii).

We now consider the weak-coupling and short-time limits. In the weak-coupling limit, the following approximations hold:

$$e^{-\Gamma(t)}\left(G(t)+1\right) \simeq 1 - \int_0^t \gamma_1(t')\,dt', \tag{36}$$

$$e^{-\Gamma(t)}G(t) \simeq \int_0^t \gamma_2(t')\,dt'. \tag{37}$$

Using these approximations, a straightforward calculation shows that conditions (i)–(ii) and (iv) reduce to

$$\text{i)} \quad \int_0^t \gamma_2(t')\,dt' \ge 0, \tag{39}$$

$$\text{ii)} \quad \int_0^t \gamma_1(t')\,dt' \ge 0, \tag{40}$$

$$\text{iv)} \quad \int_0^t \gamma_3(t')\,dt' \ge 0. \tag{41}$$

For the short-time approximation, by considering the Taylor expansion around $t = 0$ of the exponential terms $e^{-\Gamma(t)}$ and $e^{-\Gamma(t)}G(t)$, one can readily verify that the CP conditions reduce to

$$\text{i)} \quad \gamma_1(0) \ge 0, \tag{B.27}$$

$$\text{ii)} \quad \gamma_2(0) \ge 0, \tag{B.28}$$

$$\text{iv)} \quad \gamma_3(0) \ge 0. \tag{B.29}$$

for all $t \ge 0$ [110]. This condition ensures that the quantum state remains physical throughout the evolution and that the dynamical map can be represented as a sum of completely positive operators.

For the dissipative channel with Lorentzian spectral density (15), the decay function

$$f(t) = -2\,\mathrm{Re}\left[\frac{\dot{C}(t)}{C(t)}\right]$$

must remain non-negative. Consequently, the dissipative rates

$$\frac{\gamma_1(t)}{2} = (\bar{n}+1)f(t), \qquad \frac{\gamma_2(t)}{2} = \bar{n}\,f(t),$$

remain positive whenever $f(t) \ge 0$. This condition is fulfilled when the spectral width λ is sufficiently large compared to the effective coupling strength γ. In our parameter regime, where $R = \gamma/\lambda$ is either small (weak-coupling regime) or large but still compatible with positivity, we verified numerically that

$$f(t) \ge 0$$

throughout the entire evolution for all cases considered.

For the Ohmic dephasing channel with spectral density given in Equation (22), the dephasing rate $\gamma_3(t)$ is given by Equation (21):

$$\gamma_3(t) = \int_0^\infty d\omega\, J_{\mathrm{deph}}(\omega)\coth\left(\frac{\hbar\omega}{2k_B T_2}\right)\frac{\sin(\omega t)}{\omega}.$$

Since

$$\coth\left(\frac{\hbar\omega}{2k_B T_2}\right) > 0$$

for all frequencies and temperatures, and the Ohmic spectral density

$$J_{\mathrm{deph}}(\omega) = \alpha\omega e^{-\omega/\omega_c}$$

is positive definite, the integrand in Equation (21) preserves positivity. The time dependence of $\gamma_3(t)$ reflects the non-Markovian nature of the dephasing dynamics; nevertheless, complete positivity is maintained as long as the spectral density remains physical [44].

Moreover, within the short-time approximation, the complete positivity conditions reduce to

$$\gamma_1(0) \ge 0, \qquad \gamma_2(0) \ge 0, \qquad \gamma_3(0) \ge 0.$$

Using the integro-differential equation for the coherence function $C(t)$, one finds that

$$\dot{C}(0) = 0,$$

which immediately yields

$$f(0) = 0.$$

Therefore,

$$\gamma_1(0) = 0, \qquad \gamma_2(0) = 0.$$

In addition, since

$$\sin(\omega t)\Big|_{t=0} = 0,$$

the dephasing rate also satisfies

$$\gamma_3(0) = 0.$$

Hence, the short-time CP conditions are exactly satisfied for both the unmodulated case ($d = 0$) and the frequency-modulated case ($d = 2.40483\,\Omega$), for all thermal occupation numbers considered in this work.

For more general criteria concerning time-dependent master equations and complete positivity, we refer the reader to Ref. [110].

Appendix C: Canonical form of Master Equation

A general time-local master equation can always be written in the form [114, 115]

$$\dot{\rho}_q(t) = \Lambda_t[\rho_q(t)] = \sum_k A_k(t)\rho_q(t)B_k^\dagger(t), \tag{C.1}$$

where Λ_t is a linear map such that $\Lambda_t[\rho]$ is Hermitian and traceless for any Hermitian, trace-preserving density matrix ρ_q.

For a Hilbert space of dimension d, we introduce a complete, orthonormal set of $N = d^2$ basis operators $\{G_m;\ m = 0, 1, 2, \ldots, N\}$ satisfying the properties

$$G_0 = \hat{I}/\sqrt{d}, \quad G_n = G_n^\dagger, \quad \mathrm{Tr}[G_m G_n] = \delta_{mn}, \tag{C.2}$$

where $\hat{I}$ denotes the identity. Choosing $n = 0$ in the last condition implies that

$$\mathrm{Tr}[G_m] = 0 \quad \text{for } m \neq 0. \tag{C.3}$$

For brevity, we suppress the explicit time dependence in the subsequent expressions, noting that all quantities except the fixed basis operators G_m may be time-dependent. By substituting the operators $A_k = \sum_i a_{ik} G_i$ and $B_k = \sum_j b_{jk} G_j$ in Equation (C.1) we have

$$\dot{\rho}_q = \sum_{i,j} \sum_k a_{ik} b_{jk}^* \, G_i \rho_q G_j. \tag{C.4}$$

Defining the quantities $c_{ij} = \sum_k a_{ik} b_{jk}^*$ yields the unique decomposition [114]

$$\dot{\rho}_q = \sum_{i,j=0}^{N-1} c_{ij} \, G_i \rho_q G_j. \tag{C.5}$$

Because ρ_q is a physical density matrix, it must remain Hermitian ($\rho_q = \rho_q^\dagger$), implying that

$$\dot{\rho}_q = \dot{\rho}_q^\dagger.$$

Moreover, since the basis operators satisfy $G_n = G_n^\dagger$, we obtain

$$\sum_{i,j} c_{ij} \, G_i \rho_q G_j = \sum_{i,j} c_{ij}^* \, G_j \rho_q G_i = \sum_{i,j} c_{ji}^* \, G_j \rho_q G_i. \tag{C.6}$$

By comparing both sides, it follows that

$$c_{ij} = c_{ji}^*, \tag{C.7}$$

meaning that c_{ij} are the elements of an $N \times N$ Hermitian matrix. Separating out $i = 0$ and $j = 0$, Equation (C.5) can be rewritten as

$$\dot{\rho}_q = \underbrace{\frac{c_{00}}{d}\,\rho_q}_{i=0,\, j=0} + \underbrace{\sum_{i=1}^{N-1} \frac{c_{i0}}{\sqrt{d}} \, G_i \rho_q}_{j=0} + \underbrace{\sum_{j=1}^{N-1} \frac{c_{0j}}{\sqrt{d}} \, \rho_q G_j}_{i=0} + \underbrace{\sum_{i,j=1}^{N-1} d_{ij} \, G_i \rho_q G_j}_{\text{rest } (i,j>0)}, \tag{C.8}$$

where the quantities d_{ij} (equal to c_{ij}) are the elements of an $(N-1) \times (N-1)$ Hermitian "decoherence" matrix d.

Let us now split the first term, $\frac{c_{00}}{d}\,\rho$, into two equal terms so that one half can be grouped with the terms on the left and the other half with the terms on the right:

$$\dot{\rho}_q = \left(\frac{1}{2}\frac{c_{00}}{d}\rho_q + \sum_{i=1}^{N-1} \frac{c_{i0}}{\sqrt{d}} \, G_i \rho_q \right) + \left(\frac{1}{2}\frac{c_{00}}{d}\rho_q + \sum_{j=1}^{N-1} \frac{c_{0j}}{\sqrt{d}} \, \rho_q G_j \right) + \sum_{i,j=1}^{N-1} d_{ij} \, G_i \rho_q G_j. \tag{C.9}$$

Defining

$$C := \frac{1}{2}\left(\frac{c_{00}}{d} + \sum_i \sqrt{d}\, c_{i0} \, G_i \right),$$

and using that c_{00} is real and $c_{0j} = c_{j0}^*$, Equation (C.9) reduces to

$$\dot{\rho}_q = C\rho_q + \rho_q C^\dagger + \sum_{i,j=1}^{N-1} d_{ij} \, G_i \rho_q G_j. \tag{C.10}$$

Using the cyclic property of the trace, $\mathrm{Tr}[ABC] = \mathrm{Tr}[CAB]$, and applying the condition $\mathrm{Tr}[\dot{\rho}_q] = 0$,

$$\mathrm{Tr}\left[\left(C + C^\dagger + \sum_{i,j\neq 0} d_{ij} \, G_j G_i \right) \rho_q \right] = 0. \tag{C.11}$$

we obtain

$$C + C^\dagger = -\sum_{i,j=1}^{N-1} d_{ij} \, G_j G_i. \tag{C.12}$$

The time-local master equation is therefore, with $H = -2i(C - C^\dagger)$,

$$\begin{aligned} \dot{\rho}_q &= \frac{1}{2}\left[(C - C^\dagger)\rho_q + \rho_q (C^\dagger - C) + (C + C^\dagger)\rho_q + \rho_q (C^\dagger + C) \right] \\ &\quad + \sum_{i,j\neq 0} d_{ij}(t) \, G_i \rho_q G_j \\ &= -i[H, \rho_q] + \sum_{i,j\neq 0} d_{ij}(t) \left(G_i \rho_q G_j - \frac{1}{2} G_j G_i \rho_q - \frac{1}{2} \rho_q G_j G_i \right). \end{aligned} \tag{C.13}$$

Taking advantage of the Hermitian nature of the decoherence matrix d, we can rewrite it in diagonal form,

$$d_{ij} = \sum_k U_{ik} \, \gamma_k \, U_{jk}^*, \tag{C.14}$$

where U_{ik} are the eigenvectors of d, satisfying

$$\sum_k U_{ik} U_{jk}^* = \delta_{ij}, \tag{C.15}$$

and the eigenvalues γ_k of d are real but not necessarily positive at all times. Defining the time-dependent operators as follows:

$$L_k(t) := \sum_{i=1}^{N-1} U_{ik}(t) \, G_i. \tag{C.16}$$

the canonical form of Equation (C.13) is given by [100, 114, 115]

$$\begin{aligned} \dot{\rho}_q &= -i[H(t), \rho_q] \\ &\quad + \sum_{k=1}^{N-1} \gamma_k(t) \left[L_k(t)\rho_q L_k^\dagger(t) - \tfrac{1}{2} L_k^\dagger(t) L_k(t) \rho_q - \tfrac{1}{2} \rho_q L_k^\dagger(t) L_k(t) \right]. \end{aligned} \tag{C.17}$$

where the operators $L_k(t)$ form an orthonormal basis of traceless operators, i.e.,

$$\mathrm{Tr}[L_k(t)] = 0, \qquad \mathrm{Tr}[L_j^\dagger(t)\, L_k(t)] = \delta_{jk}, \tag{C.18}$$

and $H(t)$ is Hermitian. Equation (C.17) can be recognized as a Lindblad-type form, with the important distinction that the the Lindblad operators $L_k(t)$ are traceless and generally time-dependent. Moreover, the relaxation rates $\gamma(t)$ are also time-dependent and are not necessarily positive at all times.

In our model, we have a two-level ($N = 3$) system which interacts with a two reservoirs of field modes. where $H(t) = \omega(t)\sigma_z = \frac{\hbar}{2}(\omega_0 + \delta\cos(\Omega t))\sigma_z$, with time-independent Lindblad operators $L_1 = \sigma_-, L_1 = \sigma_+$ and $L_1 = \sigma_z$ and the time-dependent rates $\gamma_i(t); i = 1, 2, 3$. These constitute the complete positivity conditions for a general phase-covariant qubit dynamical map.

References

1. A. Leggett, "Macroscopic Quantum Systems and the Quantum Theory of Measurement," *Progress of Theoretical Physics Supplement* 69 (1980): 80.

2. Y. Yao, X. Xiao, L. Ge, and C. Sun, "Quantum Coherence in Multipartite Systems," *Physical Review A* 92 (2015): 022112.

3. A. Streltsov, U. Singh, H. S. Dhar, M. N. Bera, and G. Adesso, "Measuring Quantum Coherence with Entanglement," *Physical Review Letters* 115 (2015): 020403.

4. X. Hu, A. Milne, B. Zhang, and H. Fan, "Quantum Coherence of Steered States," *Scientific Reports* 6, no. 1 (2016): 1–8.

5. C. Radhakrishnan, M. Parthasarathy, S. Jambulingam, and T. Byrnes, "Distribution of Quantum Coherence in Multipartite Systems," *Physical Review Letters* 116 (2016): 150504.

6. J. Ma, B. Yadin, D. Girolami, V. Vedral, and M. Gu, "Converting Coherence to Quantum Correlations," *Physical Review Letters* 116 (2016): 160407.

7. A. Malvezzi, G. Karpat, B. Çakmak et al., "Quantum Correlations and Coherence in Spin-1 Heisenberg Chains," *Physical Review B* 93 (2016): 184428.

8. Y. C. Li and H. Q. Lin, "Quantum Coherence and Quantum Phase Transitions," *Scientific Reports* 6 (2016): 26365.

9. J. J. Chen, J. Cui, Y. R. Zhang, and H. Fan, "Coherence Susceptibility as a Probe of Quantum Phase Transitions," *Physical Review A* 94 (2016): 022112.

10. M. L. Hu and H. Fan, "Relative Quantum Coherence, Incompatibility, and Quantum Correlations of States," *Physical Review A* 95 (2017): 052106.

11. M. L. Hu, X. Hu, J. Wang et al., "Quantum Coherence and Geometric Quantum Discord," *Physics Reports* 762 (2018): 1–100.

12. E. Chitambar and G. Gour, "Comparison of Incoherent Operations and Measures of Coherence," *Physical Review A* 94 (2016): 052336.

13. C. Napoli, T. R. Bromley, M. Cianciaruso et al., "Robustness of Coherence: An Operational and Observable Measure of Quantum Coherence," *Physical Review Letters* 116 (2016): 150502.

14. S. Rana, P. Parashar, and M. Lewenstein, "Trace-Distance Measure of Coherence," *Physical Review A* 93 (2016): 012110.

15. X. D. Yu, D. J. Zhang, G. Xu, and D. Tong, "Alternative Framework for Quantifying Coherence," *Physical Review A* 94 (2016): 060302.

16. A. Streltsov, G. Adesso, and M. B. Plenio, "Colloquium: Quantum Coherence as a Resource," *Reviews of Modern Physics* 89 (2017): 041003.

17. T. Baumgratz, M. Cramer, and M. B. Plenio, "Quantifying Coherence," *Physical Review Letters* 113 (2014): 140401.

18. A. Winter and D. Yang, "Operational Resource Theory of Coherence," *Physical Review Letters* 116 (2016): 120404.

19. E. Chitambar and M. H. Hsieh, "Relating the Resource Theories of Entanglement and Quantum Coherence," *Physical Review Letters* 117 (2016): 020402.

20. V. Giovannetti, S. Lloyd, and L. Maccone, "Quantum-Enhanced Measurements: Beating the Standard Quantum Limit," *Science* 306, no. 5700 (2004): 1330–1336.

21. R. Demkowicz-Dobrzański and L. Maccone, "Using Entanglement Against Noise in Quantum Metrology," *Physical Review Letters* 113 (2014): 250801.

22. K. Sun, Z. H. Liu, Y. Wang et al., "Activation of Indistinguishability-Based Quantum Coherence for Enhanced Metrological Applications with Particle Statistics Imprint," *Proceedings of the National Academy of Sciences* 119, no. 21 (2022): e2119765119.

23. J. K. Asbóth, J. Calsamiglia, and H. Ritsch, "Computable Measure of Nonclassicality for Light," *Physical Review Letters* 94 (2005): 173602.

24. C. H. Bennett and S. J. Wiesner, "Communication via One-and Two-Particle Operators on Einstein-Podolsky-Rosen States," *Physical Review Letters* 69 (1992): 2881.

25. R. Laflamme, C. Miquel, J. P. Paz, and W. H. Zurek, "Perfect Quantum Error Correcting Code," *Physical Review Letters* 77 (1996): 198.

26. M. B. Plenio, V. Vedral, and P. L. Knight, "Quantum Error Correction in the Presence of Spontaneous Emission," *Physical Review A* 55 (1997): 67.

27. A. K. Ekert, "Quantum Cryptography Based on Bell's Theorem," *Physical Review Letters* 67 (1991): 661.

28. W. G. Unruh, "Maintaining Coherence in Quantum Computers," *Physical Review A* 51 (1995): 992.

29. L. M. Duan and G. C. Guo, "Preserving Coherence in Quantum Computation by Pairing Quantum Bits," *Physical Review Letters* 79 (1997): 1953.

30. X. Wang, "Entanglement in the Quantum Heisenberg XY Model," *Physical Review A* 64 (2001): 012313.

31. M. Arnesen, S. Bose, and V. Vedral, "Natural Thermal and Magnetic Entanglement in the 1D Heisenberg Model," *Physical Review Letters* 87 (2001): 017901.

32. V. Giovannetti, S. Lloyd, and L. Maccone, "Advances in Quantum Metrology," *Nature Photonics* 5, no. 4 (2011): 222–229.

33. J. Joo, W. J. Munro, and T. P. Spiller, "Quantum Metrology with Entangled Coherent States," *Physical Review Letters* 107 (2011): 083601.

34. J. Liu, X. Jing, and X. Wang, "Phase-Matching Condition for Enhancement of Phase Sensitivity in Quantum Metrology," *Physical Review A* 88 (2013): 042316.

35. R. Chaves, J. Brask, M. Markiewicz, J. Kołodyński, and A. Acín, "Noisy Metrology Beyond the Standard Quantum Limit," *Physical Review Letters* 111 (2013): 120401.

36. Y. Zhang, X. Li, W. Yang, and G. Jin, "Quantum Fisher Information of Entangled Coherent States in the Presence of Photon Loss," *Physical Review A* 88 (2013): 043832.

37. S. Alipour, M. Mehboudi, and A. Rezakhani, "Quantum Metrology in Open Systems: Dissipative Cramér-Rao Bound," *Physical Review Letters* 112 (2014): 120405.

38. X. M. Lu, S. Yu, and C. Oh, "Robust Quantum Metrological Schemes Based on Protection of Quantum Fisher Information," *Nature Communications* 6 (2015): 7282.

39. L. A. Correa, M. Mehboudi, G. Adesso, and A. Sanpera, "Individual Quantum Probes for Optimal Thermometry," *Physical Review Letters* 114 (2015): 220405.

40. T. Baumgratz and A. Datta, "Quantum Enhanced Estimation of a Multidimensional Field," *Physical Review Letters* 116 (2016): 030801.

41. J. Liu and H. Yuan, "Quantum Parameter Estimation with Optimal Control," *Physical Review A* 96 (2017): 012117.

42. S. Y. Liu and H. Fan, "The Application of Quantum Coherence as a Resource," *Chinese Physics B* 32 (2023): 110304.

43. F. Shahandeh, A. P. Lund, and T. C. Ralph, "Quantum Correlations and Global Coherence in Distributed Quantum Computing," *Physical Review A* 99 (2019): 052303.

44. H. P. Breuer and F. Petruccione, *The Theory of Open Quantum Systems* (Oxford University Press on Demand, 2002).

45. W. H. Zurek, "Decoherence and the Transition from Quantum to Classical," *Physics Today* 44, no. 10 (1991): 36–44.

46. W. H. Zurek and J. P. Paz, "Decoherence, Chaos, and the Second Law," *Physical Review Letters* 72 (1994): 2508.

47. R. Lo Franco, B. Bellomo, S. Maniscalco, and G. Compagno, "Dynamics of Quantum Correlations in Two-Qubit Systems Within Non-Markovian Environments," *International Journal of Modern Physics B* 27 (2013): 1345053.

48. A. Mortezapour, G. Naeimi, and R. Lo Franco, "Coherence and Entanglement Dynamics of Vibrating Qubits," *Optics Communications* 424 (2018): 26–31.

49. M. Scala, B. Militello, A. Messina et al., "Population Trapping Due to Cavity Losses," *Physical Review A* 77 (2008): 043827.

50. L. Viola and S. Lloyd, "Dynamical Suppression of Decoherence in Two-State Quantum Systems," *Physical Review A* 58 (1998): 2733.

51. M. P. Branderhorst, P. Londero, P. Wasylczyk et al., "Coherent Control of Decoherence," *Science* 320, no. 5876 (2008): 638–643.

52. R. Lo Franco, A. D'Arrigo, G. Falci, G. Compagno, and E. Paladino, "Spin-Echo Entanglement Protection from Random Telegraph Noise," *Physica Scripta* 2013, no. T153 (2013): 014043.

53. J. Tan, T. H. Kyaw, and Y. Yeo, "Non-Markovian Environments and Entanglement Preservation," *Physical Review A* 81 (2010): 062119.

54. M. Scala, R. Migliore, A. Messina, and L. Sánchez-Soto, "Robust Stationary Entanglement of Two Coupled Qubits in Independent Environments," *European Physical Journal D* 61 (2011): 199–205.

55. S. B. Xue, R. B. Wu, W. M. Zhang et al., "Decoherence Suppression via Non-Markovian Coherent Feedback Control," *Physical Review A* 86 (2012): 052304.

56. A. D'Arrigo, R. Lo Franco, G. Benenti, E. Paladino, and G. Falci, "Recovering Entanglement by Local Operations," *Annals of Physics* 350 (2014): 211–224.

57. Z. X. Man, Y. J. Xia, and N. B. An, "Enhancing Entanglement of Two Qubits Undergoing Independent Decoherences by Local Pre-and Postmeasurements," *Physical Review A* 86 (2012): 052322.

58. M. W. Noel, W. Griffith, and T. Gallagher, "Frequency-Modulated Excitation of a Two-Level Atom," *Physical Review A* 58 (1998): 2265.

59. X. Zhang, H. Jiang, J. Rao, and B. Li, "Frequency-Modulated Excitation of Potassium Atoms," *Physical Review A* 68 (2003): 025401.

60. M. Silveri, J. Tuorila, E. Thuneberg, and G. Paraoanu, "Quantum Systems Under Frequency Modulation," *Reports on Progress in Physics* 80 (2017): 056002.

61. A. Mortezapour and R. Lo Franco, "Protecting Quantum Resources via Frequency Modulation of Qubits in Leaky Cavities," *Scientific Reports* 8 (2018): 14304.

62. M. Hadipour, N. N. Yousefi, A. Mortezapour et al., "Amplified Quantum Battery via Dynamical Modulation," *Scientific Reports* 15 (2025): 14578.

63. A. Nourmandipour and A. Mortezapour, "Frequency-Modulated Qubits in a Dissipative Cavity: Entanglement Dynamics and Protection," *Quantum Information Processing* 22 (2023): 254.

64. A. Rajabalinia, M. Khazaei Shadfar, F. Nosrati et al., "Quantumness and Speedup Limit of a Qubit Under Transition-Frequency Modulation," *Physical Review A* 106 (2022): 062431.

65. A. H. Houshmand Almani, A. Mortezapour, and A. Nourmandipour, "Enhancing Quantum Synchronization in a Driven Qubit System Coupled to a Structured Environment," *Annalen der Physik* 537 (2025): 2400441.

66. M. Forozesh, A. Mortezapour, and A. Nourmandipour, "Controlling Qubit-Photon Entanglement, Entanglement Swapping and Entropic Uncertainty via Frequency Modulation," *The European Physical Journal Plus* 136 (2021): 778.

67. P. Alsing, D. S. Guo, and H. Carmichael, "Dynamic Stark Effect for the Jaynes-Cummings System," *Physical Review A* 45 (1992): 5135.

68. S. N. Shevchenko, S. Ashhab, and F. Nori, "Landau-Zener-Stückelberg Interferometry," *Physics Reports* 492, no. 1 (2010): 1–30.

69. P. M. Poggi, F. C. Lombardo, and D. A. Wisniacki, "Driving-Induced Amplification of Non-Markovianity in Open Quantum Systems Evolution," *EPL (Europhysics Letters)* 118 (2017): 20005.

70. I. Martin, G. Refael, and B. Halperin, "Topological Frequency Conversion in Strongly Driven Quantum Systems," *Physical Review X* 7 (2017): 041008.

71. H. Gray, R. Whitley, and C. Stroud, "Coherent Trapping of Atomic Populations," *Optics Letters* 3, no. 6 (1978): 218–220.

72. H. L. Carrion, O. Rojas, C. Filgueiras, and M. Rojas, "Decoherence Effects on Local Quantum Fisher Information and Quantum Coherence in a Spin-1/2 Ising-XYZ Chain," *arXiv preprint arXiv:2406.10142* (2024).

73. Z. Huang and H. Situ, "Optimal Protection of Quantum Coherence in Noisy Environment," *International Journal of Theoretical Physics* 56 (2017): 503–513.

74. C. Wellard and L. Hollenberg, "Thermal Noise in a Solid State Quantum Computer," *Journal of Physics D: Applied Physics* 35 (2002): 2499.

75. S. Simbierowicz, M. Borrelli, V. Monarkha, V. Nuutinen, and R. E. Lake, "Inherent Thermal-Noise Problem in Addressing Qubits," *PRX Quantum* 5 (2024): 030302.

76. J. Kim, J. Murugan, J. Olle, and D. Rosa, "Operator Delocalization in Quantum Networks," *Physical Review A* 105, no. 1 (2022): L010201.

77. R. Y. Cohen, *Thermalization of a 1-Dimensional Rydberg Gas and Entanglement Distribution Across Quantum Networks* (Université Paris Saclay (COmUE), 2017).

78. T. Yu and J. Eberly, "Quantum Open System Theory: Bipartite Aspects," *Physical Review Letters* 97 (2006): 140403.

79. H. P. Breuer, E. M. Laine, J. Piilo, and B. Vacchini, "Colloquium: Non-Markovian Dynamics in Open Quantum Systems," *Reviews of Modern Physics* 88 (2016): 021002.

80. M. A. Nielsen and I. L. Chuang, *Quantum Computation and Quantum Information* (Cambridge University Press, 2010).

81. Z. He, H. S. Zeng, Y. Chen, and C. Yao, "Non-Markovian Dynamics of a Dephasing Model in a Squeezed Thermal Bath," *Laser Physics Letters* 16 (2019): 065204.

82. J. Lankinen, H. Lyyra, B. Sokolov, et al., "Complete Positivity, Finite-Temperature Effects, and Additivity of Noise for Time-Local Qubit Dynamics," *Physical Review A* 93 (2016): 052103.

83. B. M. Garraway, "Nonperturbative Decay of an Atomic System in a Cavity," *Physical Review A* 55 (1997): 2290.

84. B. M. Garraway, "Decay of an Atom Coupled Strongly to a Reservoir," *Physical Review A* 55 (1997): 4636.

85. B. Dalton, S. M. Barnett, and B. M. Garraway, "Theory of Pseudomodes in Quantum Optical Processes," *Physical Review A* 64 (2001): 053813.

86. M. O. Scully and M. S. Zubairy, *Quantum Optics* (Cambridge University Press, 1999).

87. J. H. Reina, L. Quiroga, and N. F. Johnson, "Decoherence of Quantum Registers," *Physical Review A* 65 (2002): 032326.

88. T. Chanda and S. Bhattacharya, "Delineating Incoherent Non-Markovian Dynamics Using Quantum Coherence," *Annals of Physics* 366 (2016): 1–12.

89. J. Teittinen, H. Lyyra, B. Sokolov, and S. Maniscalco, "Revealing Memory Effects in Phase-Covariant Quantum Master Equations," *New Journal of Physics* 20 (2018): 073012.

90. G. M. Palma, K. A. Suominen, and A. Ekert, "Quantum Computers and Dissipation," *Proceedings of the Royal Society of London A* 452, no. 1946 (1996): 567–584.

91. P. Haikka, T. Johnson, and S. Maniscalco, "Non-Markovianity of Local Dephasing Channels and Time-Invariant Discord," *Physical Review A* 87 (2013): 010103.

92. F. Giraldi, "Regular Patterns in the Information Flow of Local Dephasing Channels," *Physical Review A* 95 (2017): 022109.

93. F. Giraldi, "Preparing Decoherence-Recoherence Times of a Qubit with Special Nonselective Measurement Schemes," *Open Systems and Information Dynamics* 28 (2021): 2150002.

94. V. V. Ignatyuk and C. Samorodov, "Dependence of the Recoherence Times and Recoherence Increments on the State of Phonon Bath in a Single-Qubit Dephasing Model," *Physical Review A* 112 (2025): 062213.

95. J. Tuorila, M. Silveri, M. Sillanpää et al., "Stark Effect and Generalized Bloch-Siegert Shift in a Strongly Driven Two-Level System," *Physical Review Letters* 105 (2010): 257003.

96. Y. Nakamura, Y. A. Pashkin, and J. S. Tsai, "Rabi Oscillations in a Josephson-Junction Charge Two-Level System," *Physical Review Letters* 87 (2001): 246601.

97. J. Li, M. Silveri, K. Kumar et al., "Motional Averaging in a Superconducting Qubit," *Nature Communications* 4 (2013): 1420.

98. W. D. Oliver, Y. Yu, J. C. Lee et al., "Mach-Zehnder Interferometry in a Strongly Driven Superconducting Qubit," *Science* 310, no. 5754 (2005): 1653–1657.

99. G. Cao, H. O. Li, T. Tu, et al., "Ultrafast Universal Quantum Control of a Quantum-Dot Charge Qubit Using Landau-Zener-Stückelberg Interference," *Nature Communications* 4 (2013): 1401.

100. H. P. Breuer, E. M. Laine, and J. Piilo, "Measure for the Degree of Non-Markovian Behavior of Quantum Processes in Open Systems," *Physical Review Letters* 103 (2009): 210401.

101. J. Piilo, S. Maniscalco, K. Härkönen, and K. A. Suominen, "Non-Markovian Quantum Jumps," *Physical Review Letters* 100 (2008): 180402.

102. B. Bylicka, D. Chruściński, and S. Maniscalco, "Non-Markovianity and Reservoir Memory of Quantum Channels: A Quantum Information Theory Perspective," *Scientific Reports* 4 (2014): 5720.

103. A. W. Chin, S. F. Huelga, and M. B. Plenio, "Quantum Metrology in Non-Markovian Environments," *Physical Review Letters* 109 (2012): 233601.

104. B. H. Liu, L. Li, Y. F. Huang, et al., "Experimental Control of the Transition From Markovian to Non-Markovian Dynamics of Open Quantum Systems," *Nature Physics* 7, no. 12 (2011): 931–934.

105. C. Addis, G. Brebner, P. Haikka, and S. Maniscalco, "Coherence Trapping and Information Backflow in Dephasing Qubits," *Physical Review A* 89 (2014): 024101.

106. P. Haikka, J. Goold, S. McEndoo, F. Plastina, and S. Maniscalco, "Non-Markovianity, Loschmidt Echo, and Criticality: A Unified Picture," *Physical Review A* 85 (2012): 060101.

107. M. B. Ruskai, S. Szarek, and E. Werner, "An Analysis of Completely-Positive Trace-Preserving Maps on M2," *Linear Algebra and its Applications* 347, no. 1–3 (2002): 159–187.

108. M. J. Hall, "Complete Positivity for Time-Dependent Qubit Master Equations," *Journal of Physics A: Mathematical and Theoretical* 41 (2002): 205302.

109. E. Adlam, "The Operational Choi–Jamiołkowski Isomorphism," *Entropy* 22 (2020): 1063.

110. D. Manzano, "A Short Introduction to the Lindblad Master Equation," *AIP Advances* 10, no. 2 (2020): 025106.

111. M. S. Leifer, "Conditional Density Operators and the Subjectivity of Quantum Operations," in *American Institute of Physics Conference Proceedings* 889 (2007): 172–186.

112. K. Życzkowski and I. Bengtsson, "On Duality Between Quantum Maps and Quantum States," *Open Systems and Information Dynamics* 11, no. 1 (2004): 3–42.

113. A. Fujiwara and P. Algoet, "One-to-One Parametrization of Quantum Channels," *Physical Review A* 59 (1999): 3290.

114. V. Gorini and A. Kossakowski and Sudarshan ECG, "Completely Positive Dynamical Semigroups of N-Level Systems," *Journal of Mathematical Physics* 17, no. 5 (1976): 821–825.

115. M. J. Hall, J. D. Cresser, L. Li, and E. Andersson, "Canonical Form of Master Equations and Characterization of Non-Markovianity," *Physical Review A* 89 (2014): 042120.